JBIC Journal of Biological Inorganic Chemistry (2022) 27:271–281
https://doi.org/10.1007/s00775-022-01932-9

ORIGINAL PAPER

New Pd(II) complexes of the bisthiocarbohydrazones derived from isatin and disubstituted salicylaldehydes: Synthesis, characterization, crystal structures and inhibitory properties against some metabolic enzymes

Yeliz Kaya[1] · Ayşe Erçağ[1] · Yunus Zorlu[2] · Yeliz Demir[3] · İlhami Gülçin[4]

Received: 23 October 2021 / Accepted: 6 February 2022 / Published online: 17 February 2022

Abstract

Pd(II) complexes (**Pd1**, **Pd2**, and **Pd3**) were synthesized for the first time using asymmetric isatin bisthiocarbohydrazone ligands and $PdCl_2(PPh_3)_2$. All complexes were characterized by a range of spectroscopic and analytical techniques. The molecular structures of **Pd1** and **Pd3** have been determined by single-crystal X-ray diffraction analysis. The complexes are diamagnetic and exhibit square planar geometry. The asymmetric isatin bisthiocarbohydrazone ligands coordinate to Pd(II) ion in a tridentate manner, through the phenolic oxygen, imine nitrogen and thiol sulfur, forming five- and six-membered chelate rings within their structures. The fourth coordination site in these complexes is occupied by PPh_3 (triphenylphosphine). The free ligands and their Pd(II) complexes were evaluated for their carbonic anhydrase I, II (hCAs) and acetylcholinesterase (AChE) inhibitor activities. They showed a highly potent inhibition effect on AChE and hCAs. K_i values are in the range of 9 ± 0.6 – 30 ± 5.4 nM for AChE, 7 ± 0.5 – 16 ± 2.2 nM for hCA I and 3 ± 0.3–24 ± 1.9 nM for hCA II isoenzyme. The results clearly demonstrated that the ligands and their Pd(II) complexes effectively inhibited the used enzymes.

Graphical abstract

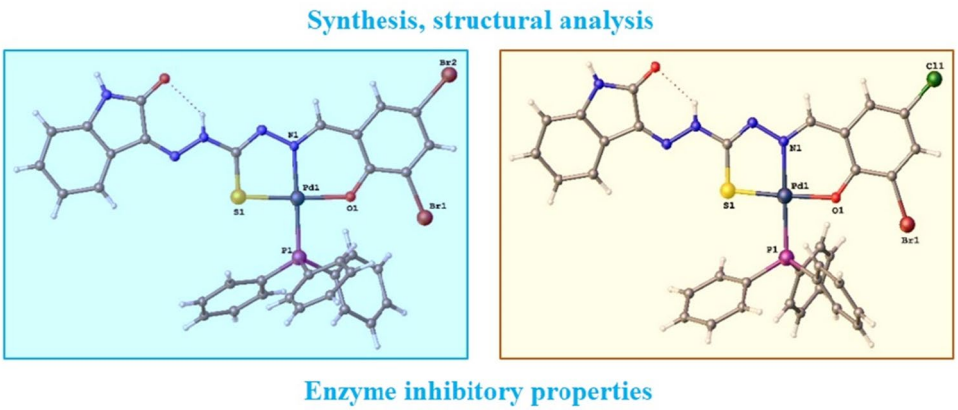

Keywords Isatin · Bisthiocarbohydrazone · Palladium(II) · Crystal structure · Carbonic anhydrase · Acetylcholinesterase

✉ Ayşe Erçağ
ercaga@istanbul.edu.tr

Extended author information available on the last page of the article

Introduction

Isatin and derivatives can inhibit many enzymes and receptors, cross the brain barrier and be used in the development of new drugs [1–3]. Isatin has been reported to be a reversible inhibitor of MAO isozyme [4]. These compounds, besides their use as pharmaceutical raw materials, are also synthetic substrates used in the synthesis of a wide variety of heterocyclic compounds [5, 6].

Thiocarbohydrazones are homologs of the thiosemicarbazones, a class of compounds that have been extensively studied for their antimicrobial, antifungal and anticancer activities and metal complexes [7, 8]. Thiocarbohydrazones containing O, N and S donor atoms are of interest due to their wide biological activity and binding to metal ions in various ways [9, 10]. In addition, the presence of additional coordination sites on the side substituents can affect both stoichiometry and metal ion selectivity [11]. Also, the asymmetry of thiocarbohydrazones can induce different metal coordination geometry [12].

N-Ethyl isatin-beta-thiocarbohydrazone has been found to exert a strong antiproliferative effect against B16 cells [13]. Isatin bisthiocarbohydrazone ligands and some metal complexes have shown promising cytotoxic activity when screened using the in vitro method [14, 15].

Despite thiocarbohydrazones as multifunctional ligands, not many studies have been carried out to evaluate the biological activity of their metal complexes. Furthermore, little data concerning the enzyme activities are found.

The search for new chemotherapy drugs that have fewer side effects and can treat cisplatinum-resistant strains has led researchers to Pd(II) complexes [16–18]. Pd(II) complexes also possess antiviral, antiinflammatory, antimalarial and antioxidant activities [19–21]. In addition, these complexes are potential inhibitors of enzymes [22, 23]. These properties have aroused interest in the design of Pd(II) complexes.

Phosphine ligands used as a secondary ligand in this work have the ability to act as both σ-bases and π-acids [24]. The use of a bulky ligand such as PPh_3 in the structure increases the stability of Pd(II) complexes and prevents them from being easily dissociated in the solution [25].

Carbonic anhydrase catalyzes the hydration of carbon dioxide and water to proton and bicarbonate ions [26, 27]. The reaction has a key role in several pathological and physiological reactions related to fluid secretion, calcification, tumorigenicity, pH control, ion transportation and biosynthetic reactions including ureagenesis, lipogenesis and gluconeogenesis [28–30]. The inhibition of these zinc containing enzymes is a crucial target associated with the treatment of many disorders such as epilepsy, obesity, and glaucoma [31–33]. CA inhibition was also foreseen as a novel approach to combat metastases and tumors [34, 35]. So, these isoenzymes are crucial targets for the design and synthesis of novel inhibitors with clinical applications [36, 37]. On the other hand, a reduction in cholinergic neurons in the basal forebrain has been associated with decreased acetylcholine (ACh) release [38, 39]. The enzyme acetylcholinesterase (AChE) can impair memory and lower levels of ACh in the brain, hallmarks of Alzheimer's disease (AD). AChE inhibitors can inhibit ACh hydrolysis by reducing the level of AChE [40–42]. AChE inhibitors have been proposed for the symptomatic treatment of mild to moderate AD [43, 44].

In our previous study, we reported the synthesis and spectral characterization of new asymmetric isatin bisthiocarbohydrazone ligands (**1**, **2**, and **3**) and their Ni(II) complexes [45]. The present paper describes the synthesis and spectral studies of new mixed ligand Pd(II) complexes (**Pd1**, **Pd2** and **Pd3**) of the asymmetric isatin bisthiocarbohydrazone ligands derived from 3,5-disubstituted salicylaldehydes. The study also defines the single crystal structures of the **Pd1** and **Pd3** complexes. Finally, here for the first time, detailed in vitro enzyme inhibitor activities of the asymmetric isatin bisthiocarbohydrazone ligands and their Pd(II) complexes are reported.

Experimental

Materials

Thiocarbohydrazide was synthesized as described in the literature [46]. Isatin, carbon disulfide, hydrazine hydrate, 3,5-dichlorosalicylaldehyde, 3-bromo-5-chlorosalicylaldehyde, 3,5-dibromosalicylaldehyde, bis(triphenylphosphine) palladium(II) dichloride [$PdCl_2(PPh_3)_2$], and solvents were used as received from Sigma Aldrich, Alfa Aesar and Merck chemical companies.

Physical measurements

Elemental analysis (C, H, N and S) was carried out using a Thermo Finnigan Flash EA 1112 Series Elemental Analyzer. The electronic spectra were recorded on a Shimadzu 2600 UV–Vis Spectrophotometer in DMF. Infrared spectra were taken on an Agilent Cary 630 FTIR spectrometer using ATR (Attenuated Total Reflectance) technic in the 4000–650 cm^{-1} range. ^{1}H and ^{31}P NMR spectra were recorded in DMSO-d_6 on a Varian UNITY INOVA 500 MHz NMR spectrometer at room temperature. The mass spectra were recorded on a Thermo Finnigan LCQ Advantage MAX system using ESI (Electrospray Ionization) as the ionization technique. The

X-ray data were obtained with a Bruker APEX II CCD three-circle diffractometer. The magnetic measurements were carried out at room temperature by the Gouy technique with a MK I model device obtained from Sherwood Scientific. The molar conductivities of the complexes in DMSO (10^{-3} M) were measured on a digital WPA CMD 750 conductivity meter at room temperature.

Synthesis of isatin monothiocarbohydrazone

Isatin monothiocarbohydrazone was prepared according to a known method with minor modifications [13].

[1-(2-oxoindolin-3-ylidene)thiocarbohydrazone]: Yield: 85%. Color: orange. M.p.: 240–241 °C. Anal. calcd. for $C_9H_9N_5OS$ (235.26 g/mol): C 45.95, H 3.86, N 29.77, S 13.63%. Found: C 45.34, H 3.71, N 29.56, S 13.62%. FT-IR (cm^{-1}): $\nu(NH_2)$ 3290 and 3240, ν(NH) 3168 and 3127, ν(C=N) 1616, $\nu(C=O)_{isatin}$ 1687, ν(C=S) 1269. ^{1}H NMR (500 MHz, DMSO-d_6, ppm) δ: 12.44 (s, 1H, NH), 11.15 (s, 1H, isatin NH), 10.71 (s, 1H, NH), 7.67–6.91 (m, 4H, aromatic H), 5.13 (s, 2H, NH_2). UV–Vis (DMF) [λ_{max} (nm)]: 265, 277, 362.

Synthesis of asymmetric isatin bisthiocarbohydrazone ligands

The asymmetric isatin bisthiocarbohydrazone ligands (**1**–**3**) were synthesized from isatin monothiocarbohydrazone using 3,5-dibromosalicylaldehyde, 3,5-dichlorosalicylaldehyde, and 3-bromo-5-chlorosalicylaldehyde, respectively, according to our previously published procedure [45].

1-[2-oxoindolin-3-ylidene]-5-[3,5-dibromo-2-hydroxyphenyl)methylidene]thiocarbohydrazone, (1): Yield: 78%. Color: Orange. M.p.: 246–247 °C. Anal. calcd. for $C_{16}H_{11}Br_2N_5O_2S.C_3H_7NO$ (570.26 g/mol): C 40.02, H 3.18, N 14.74, S 5.62%. Found: C 40.34, H 3.25, N 14.63, S 5.86%. FT-IR (cm^{-1}): ν(OH) 3214, ν(NH) 3176 and 3138, ν(C=N) 1618 and 1604, $\nu(C=O)_{isatin}$ 1694, $\nu(C=O)_{DMF}$ 1649, ν(C=S) 1270. ^{1}H NMR (500 MHz, DMSO-d_6, ppm) δ: 14.54, 13.09 (s, isomer ratio: 1/1, 1H, OH); 11.39, 11.32 (s, isomer ratio: 1/1, 1H, isatin NH); 12.67, 12.53 (s, isomer ratio: 1/1, 1H, NH); 13.02, 10.16 (s, isomer ratio: 1/1, 1H, NH); 8.79, 8.50 (s, isomer ratio: 1/1, 1H, CH=N); 7.95 [s, 1H, $(CH=O)_{DMF}$]; 8.18–6.93 (m, 6H, aromatic H); 2.89 [s, 3H, $(CH_3)_{DMF}$]; 2.73 [s, 3H, $(CH_3)_{DMF}$]. UV–Vis (DMF) [λ_{max} (nm)]: 265, 286, 375, 458. *m/z* (+c ESI–MS): 497.9 ([M-DMF]$^+$, 16.84%), *m/z* (+c ESI–MS): 254.8 ([M−$C_{13}H_{14}N_6O_2S$+3H]$^+$, 100%).

1-[2-oxoindolin-3-ylidene]-5-[3,5-dichloro-2-hydroxyphenyl)methylidene]thiocarbohydrazone, (2): Yield: 76%. Color: Orange. M.p.: 278–280 °C. Anal. calcd. for $C_{16}H_{11}Cl_2N_5O_2S.C_3H_7NO$ (481.35 g/mol): C 47.41, H 3.77, N 17.46, S 6.66%. Found: C 47.30, H 3.85, N 17.32, S 6.81%. FT-IR (cm^{-1}): ν(OH) 3215, ν(NH) 3171 and 3136, ν(C=N) 1619 and 1597, $\nu(C=O)_{isatin}$ 1694, $\nu(C=O)_{DMF}$ 1651, ν(C=S) 1269. ^{1}H NMR (500 MHz, DMSO-d_6, ppm) δ: 14.58, 13.09 (s, isomer ratio: 1/1, 1H, OH); 11.39, 11.31 (s, isomer ratio: 1/1, 1H, isatin NH); 12.68, 12.38 (s, isomer ratio: 1/1, 1H, NH); 13.00, 10.32 (s, isomer ratio: 1/1, 1H, NH); 8.82, 8.52 (s, isomer ratio: 1/1, 1H, CH=N); 7.95 [s, 1H, $(CH=O)_{DMF}$]; 8.07–6.93 (m, 6H, aromatic 6H); 2.89 [s, 3H, $(CH_3)_{DMF}$]; 2.73 [s, 3H, $(CH_3)_{DMF}$]. UV–Vis (DMF) [λ_{max} (nm)]: 265, 285, 375, 453.

1-[2-oxoindolin-3-ylidene]-5-[3-bromo-5-chloro-2-hydroxyphenyl)methylidene]thiocarbo-hydrazone, (3): Yield: 81%. Color: orange. M.p.: 250–251 °C. Anal. calcd. for $C_{16}H_{11}BrClN_5O_2S.C_3H_7NO$ (525.81 g/mol): C 43.40, H 3.45, N 15.98, S 6.10%. Found: C 43.52, H 3.28, N 15.83, S 6.26%. FT-IR (cm^{-1}): ν(OH) 3212, ν(NH) 3171 and 3135, ν(C=N) 1617 and 1596, $\nu(C=O)_{isatin}$ 1693, $\nu(C=O)_{DMF}$ 1648, ν(C=S) 1268. ^{1}H NMR (500 MHz, DMSO-d_6, ppm) δ: 14.57, 13.09 (s, isomer ratio: 1/1, 1H, OH); 11.40, 11.32 (s, isomer ratio: 1/1, 1H, isatin NH); 12.68, 12.51 (s, isomer ratio: 1/1, 1H, NH); 13.02, 10.14 (s, isomer ratio: 1/1, 1H, NH); 8.80, 8.51 (s, isomer ratio: 1/1, 1H, CH=N); 7.95 [s, 1H, $(CH=O)_{DMF}$]; 7.94–6.90 (m, 6H, aromatic 6H); 2.86 [s, 3H, $(CH_3)_{DMF}$]; 2.70 [s, 3H, $(CH_3)_{DMF}$]. UV–Vis (DMF) [λ_{max} (nm)]: 265, 287, 375, 456.

Synthesis of Pd(II) complexes

The Pd(II) complexes were prepared using the general procedure as given below.

1 mmol of ligand (**1**–**3**) was dissolved in 10 mL of methanol and 10 mL of DCM. Then, 1 mmol of $PdCl_2(PPh_3)_2$ was added to this solution and the mixture was refluxed for 5 h. The dark orange product was filtered. The precipitate was washed with methanol and dried in a vacuum.

[Pd(1)PPh_3], (Pd1): Yield: 61%. Color: dark orange. M.p.: 318–319 °C. Anal. calcd. for $C_{34}H_{24}Br_2N_5O_2PPdS$ (863.85 g/mol): C 47.27, H 2.80, N 8.11, S 3.71%. Found: C 47.33, H 2.69, N 8.17, S 3.63%. FT-IR (cm^{-1}): ν(NH) 3226, ν(C=N) 1617 and 1591, $\nu(C=O)_{isatin}$ 1684, $\nu(PPh_3)$ 1434, 1096, 734, 689. ^{1}H NMR (500 MHz, DMSO-d_6, ppm) δ: 13.27 (s, 1H, NH), 11.20 (s, 1H, isatin NH), 8.77 (s, 1H, CH=N), 7.84–6.89 (m, 21H, aromatic H). ^{31}P NMR (500 MHz, DMSO-d_6, ppm) δ: 23.42. UV–Vis (DMF) [λ_{max} (nm)]: 265, 301, 367, 468, 556.

[Pd(2)PPh_3], (Pd2): Yield: 58%. Color: dark orange. M.p.: 335–336 °C. Anal. calcd. for $C_{34}H_{24}Cl_2N_5O_2PPdS$ (774.95 g/mol): C 52.70, H 3.12, N 9.04, S 4.14%. Found: C 52.61, H 3.04, N 9.16, S 4.27%. FT-IR (cm^{-1}): ν(NH) 3162, ν(C=N) 1617 and 1592, $\nu(C=O)_{isatin}$ 1676, $\nu(PPh_3)$ 1427, 1095, 744, 688. ^{1}H NMR (500 MHz, DMSO-d_6, ppm) δ: 13.28 (s, 1H, NH), 11.20 (s, 1H, isatin NH), 8.78 (s, 1H, CH=N), 7.69–6.89 (m, 21H, aromatic H). ^{31}P NMR

(500 MHz, DMSO-d_6, ppm) δ: 23.12. UV–Vis (DMF) [λ_{max} (nm)]: 265, 302, 366, 467, 556. *m/z* (+c ESI–MS): 775.5 ([M+H]$^+$, 100%).

[Pd(3)PPh$_3$], (Pd3): Yield: 66%. Color: Dark orange. M.p.: 326–327 °C. Anal. calcd. for $C_{34}H_{24}BrClN_5O_2PPdS$ (819.40 g/mol): C 49.84, H 2.95, N 8.55, S 3.91%. Found: C 49.97, H 2.84, N 8.47, S 3.97%. FT-IR (cm^{-1}): ν(NH) 3192, ν(C=N) 1619 and 1587, ν(C=O)$_{isatin}$ 1681, ν(PPh$_3$) 1430, 1097, 737, 689. ^{1}H NMR (500 MHz, DMSO-d_6, ppm) δ: 13.26 (s, 1H, NH), 11.19 (s, 1H, isatin NH), 8.78 (s, 1H, CH=N), 7.73–6.89 (m, 21H, aromatic H). UV–Vis (DMF) [λ_{max} (nm)]: 265, 303, 367, 468, 557. *m/z* (+c ESI–MS): 820.0 ([M+H]$^+$, 100%).

X-ray crystallography

Single crystal X-ray diffraction data for **Pd1** and **Pd3** were collected using a Bruker APEX II CCD three-circle diffractometer. Indexing was performed using APEX2 [47]. Data integration and reduction were carried out with SAINT [48]. Absorption correction was performed by the multi-scan method implemented in SADABS [49]. All the structures were solved using SHELXT [50] and then refined by full-matrix least-squares refinements on F^2 using the SHELXL [51] in Olex2 Software Package [52]. The aromatic and aliphatic C-bound H atoms were positioned geometrically and refined using a riding mode. The N–H distances in lattice water molecule were restrained to be 0.86 A from O atom, and their positions were constrained to refine on their parent O atoms with Uiso(H) = 1.2Ueq(N). Crystal structure validations and geometrical calculations were performed using Platon software [53]. Mercury software [54] was used for the visualization of the cif file. **Pd3** displays disorder of the dimethylformamide (DMF) molecule over two sites with occupancies 0.52:0.48. Additional crystallographic data with CCDC reference numbers 2097281 (**Pd1**) and 2097282 (**Pd3**) has been deposited within the Cambridge Crystallographic Data Center via www.ccdc.cam.ac.uk/deposit.

Biological studies

hCAs and AChE inhibition assay

Both hCA isoforms were purified from human erythrocytes by sepharose-4B-L-tyrosine-sulfanilamide affinity chromatography. The inhibitory effects of asymmetric isatin bisthiocarbohydrazone ligands (**1–3**) and their Pd(II) complexes (**Pd1**–**Pd3**) on the esterase activity of the hCAs were spectrophotometrically determined at 348 nm according to Verpoorte's method [55] as described in previous studies [56, 57]. hCAs activities were measured using 4-nitrophenyl acetate as the substrate [58–60]. Also, AChE from *Electrophorus electricus* was purchased from Sigma-Aldrich Chemie GmbH. In vitro effects of the compounds (**1**–**Pd3**) on AChE activity were evaluated by Ellman's assay [61] as described in prior studies [62, 63]. The results were performed spectrophotometrically at 412 nm using acetylthiocholine iodide as a substrate as in our previous studies [64].

hCAs and AChE kinetic analysis

To study the in vitro inhibitory mechanisms of the compounds (**1**–**Pd3**), kinetic studies were performed with the variable substrate and complex concentrations, and IC_{50} plots and Lineweaver–Burk plots were generated as in our previous studies [65–67]. Half maximum inhibitory concentration (IC_{50}) is a measure of the power of newly synthesized compounds or substances to inhibit a specific biological or biochemical function. The IC_{50} is a quantitative measure of the amount of inhibitor required to inhibit a given and known enzyme activity by 50% [68]. On the other hand, the inhibitor constant (K_i) is an indicator of how potent an inhibitor is; is the concentration required to produce half-maximum inhibition. The inhibitor constant (K_i) indicates how potent an inhibitor is. It is derived from the Lineweaver–Burk plots. Low IC_{50} and K_i values indicate the high affinity inhibitor toward enzyme [69, 70]. From the observed data, IC_{50} and K_i values for these **1**–**Pd3** were calculated and the inhibition types of these compounds were determined according to previous studies [71–73].

Results and discussion

Synthesis

In this study, new asymmetric isatin bisthiocarbohydrazone ligands were prepared in two steps. First, thiocarbohydrazide and isatin react to give isatin monothiocarbohydrazone. Second, isatin monothiocarbohydrazone and respective 3,5-disubstituted salicylaldehydes react to give the asymmetric isatin bisthiocarbohydrazone ligands (**1–3**). New Pd(II) complexes (**Pd1**–**Pd3**) with mixed ligand were prepared by the reaction of the asymmetric isatin bisthiocarbohydrazone ligands and $PdCl_2(PPh_3)_2$ (Scheme 1). Asymmetric bisthiocarbohydrazones served as the dibasic tridentate ONS donor ligand and replaced it by removing two chloride ions and one triphenylphosphine molecule from the starting complex. The complexes are stable at room temperature and are very

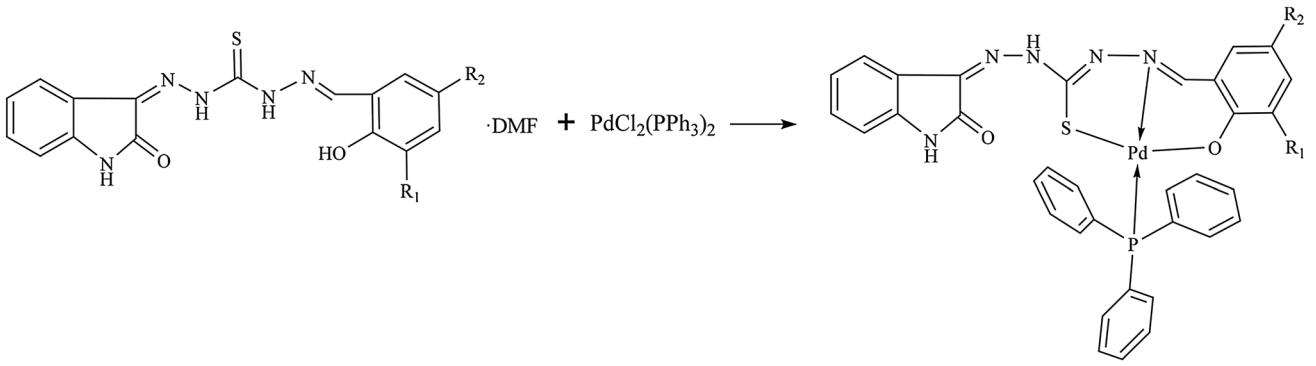

Scheme 1. Synthesis of the complexes (R^1: Br, R^2: Br for **1** and **Pd1**; R^1: Cl, R^2: Cl for **2** and **Pd2**; R^1: Br, R^2: Cl for **3** and **Pd3**)

soluble in chloroform, acetone, DCM, DMSO and DMF. Low molar conductance values (15–21 Ω^{-1} cm^2 mol^{-1}) of the complexes in 10^{-3} M DMSO indicate that their non-electrolytic nature [74, 75]. The μ_{eff} measurements show that the complexes are diamagnetic and these results reveal the square planar geometry of the Pd(II) ion [76, 77]. The elemental analyses are in good agreement with the molecular formula of the compounds.

IR spectroscopy

The fact that the band attributed to the vibration of the OH group around 3200 cm^{-1} in the IR spectra of the ligands is not observed in the complexes can be interpreted that the ligands are bound to the metal by deprotonation from the phenolic OH group. The strong bands at 3176–3135 cm^{-1} related to the stretching vibration of two NH groups in the IR spectra of ligands weakened and shifted after complexation. This shows that one of the two NH groups in the thiocarbohydrazone molecule participates in the formation of the complex. The stretching vibrations belonging to imine groups, ν(C=N), were observed at 1618 and 1604 cm^{-1} for 1, 1619 and 1597 cm^{-1} for 2, 1617 and 1596 cm^{-1} for 3. After complex formation, the frequencies of ν(C=N) changed approximately 10 cm^{-1} compared to the free ligand. These shifts are dedicated to the formation of the complex from at least one of the imine groups. ν(C=O) bands of the isatin moiety at 1694–1693 cm^{-1} observed in the ligands were also observed to be slightly displaced in the complexes. Therefore, it can be said that the isatin part of the ligand does not participate in the coordination. In the spectra of the ligands, bands attributed to ν(C=S) vibration in the 1270–1268 cm^{-1} region were not observed in the complexes. The absence of this band in the IR spectra of metal complexes suggests that the metal atom is coordinated to ligands on the sulfur atom by deprotonation. Finally, the new bands corresponding to PPh_3 ligands were observed around 1430, 1095, 740 and 689 cm^{-1} in the spectra of all complexes [15, 45, 78, 79].

^{1}H and ^{31}P NMR spectroscopies

In the ^{1}H NMR spectra of the ligands; OH (aldehyde) and NH (isatin) signals were observed as two separate singlets. Similarly, signals corresponding to two separate NH groups of thiocarbohydrazone moiety were observed around δ 12.68, 12.51 (s, isomer ratio: 1/1, 1H, NH) and δ 13.02, 10.14 (s, isomer ratio: 1/1, 1H, NH). These data indicate that the ligands exist in two isomeric forms, i.e., Z and E-forms. In the Pd(II) complexes, this isomerism disappears because the rotation of thiocarbohydrazone around its double bonds is hindered. The presence of DMF in the ligands was observed in the NMR spectra. The chemical shift observed for the OH protons in the ligands was not observed in any of the complexes. This confirms the bonding of the oxygen atoms to the metal ions (C–O–M). The signal belonging to the NH group of isatin was seen as a singlet at the almost same place in the complexes. In the spectra of the complexes, a single NH (TCH) signal around δ 13.27 ppm was observed. The disappearance of the proton in the other NH group of TCH indicates that the NH group is attached to the metal by deprotonation. All these results show that half of the ligand is involved in the formation of the complex [14, 45, 80, 81].

^{31}P NMR spectra of Pd1 and Pd2 exhibited singlets at δ 23.42 and δ 23.12 ppm, respectively, indicating one coordinated triphenylphosphine [82, 83]. ^{1}H and ^{31}P NMR spectra of the complexes are given in Figure S1–S5.

UV–Vis spectroscopy

UV–Vis spectra of the ligands and the complexes were recorded in 3×10^{-5} M DMF solution at room temperature in the region of 200–800 nm. Two absorption bands appearing at 265 and 285–287 nm in the ligands were attributed to $\pi \rightarrow \pi^*$ transitions of the benzene rings. The other bands at 375 and 453–458 nm are probably due to the $n \rightarrow \pi^*$ transitions of the azomethine groups. These transitions

of azomethine groups in the ligands shifted around 8 nm (~ 367 nm) in the complexes. This shift can be attributed to the coordination of the azomethine groups to the metal ion. In the complexes, the absorption bands at 468 nm can be assigned to the ligand charge transfer transitions (LMCT). In addition, the complexes have shown d-d bands in the visible region at 556–557 nm [45, 74, 84, 85]. UV–Vis spectra of the complexes are given in Figure S6–S8. UV–Vis spectra over time show that the complexes are stable in aqueous solutions (Figure S11).

Mass spectrometry

Mass spectra of Pd2 and Pd3 were recorded using ESI (Electrospray Ionization) as the ionization technique. In the mass spectra of Pd2 and Pd3, the base peaks were observed at *m*/*z* 775.5 and *m*/*z* 820.0 with 100% relative abundance, respectively. These peaks correspond to $[M+H]^+$ for both

Table 2 Comparison of the selected bond lengths (Å) and bond angles (°) for the complexes **Pd1** and **Pd3**

	Pd1	**Pd3**
Bond lengths (Å)		
Pd1—S1	2.2561 (13)	2.2480 (12)
Pd1—O1	2.030 (2)	2.011 (3)
Pd1—N1	2.032 (3)	2.020 (3)
Pd1—P1	2.2966 (15)	2.2781 (12)
N1—N2	1.398 (4)	1.383 (4)
N3—N4	1.338 (4)	1.341 (5)
Bond angles (°)		
S1—Pd1—P1	93.34 (3)	95.91 (4)
O1—Pd1—S1	176.58 (7)	177.13 (9)
O1—Pd1—P1	89.84 (7)	86.85 (9)
O1—Pd1—N1	91.86 (10)	92.56 (13)
N1—Pd1—S1	84.91 (8)	84.71 (10)
N1—Pd1—P1	176.80 (8)	177.62 (10)

Table 1 Crystal data and structure refinement details for **Pd1** and **Pd3**

Compound	**Pd1**	**Pd3**
CCDC	2097281	2097282
Empirical formula	$C_{34}H_{24}Br_2N_5O_2PPdS$	$C_{37}H_{31}BrClN_6O_3PPdS$
Formula weight (g mol^{-1})	863.83	892.47
Temperature (K)	298	298
Radiation	MoKα ($\lambda = 0.71073$)	MoKα ($\lambda = 0.71073$)
Crystal system	Monoclinic	Triclinic
Space group	$P2_1/n$	P-1
a (Å)	16.607 (8)	9.5263 (8)
b (Å)	9.618 (5)	14.1589 (11)
c (Å)	21.664 (11)	14.9127 (12)
α (°)	90	105.205 (2)
β (°)	111.761 (8)	106.865 (2)
γ (°)	90	90.752 (2)
Crystal size (mm)	0.28 × 0.25 × 0.13	0.31 × 0.12 × 0.05
V ($Å^3$)	3213 (3)	1848.9 (3)
Z	4	2
ρ_{calcd} (g cm^{-3})	1.786	1.603
μ (mm^{-1})	3.220	1.800
F(000)	1704	896
2*θ* range for data collection (°)	2.666–50	2.97–50.052
Index ranges	$-19 \le h \le 19, -11 \le k \le 11, -25 \le l \le 25$	$-11 \le h \le 11, -16 \le k \le 16, -17 \le l \le 17$
Reflections collected	22,837	15,616
Independent reflections	5521 [$R_{int} = 0.0354$, $R_{sigma} = 0.0307$]	6471 [$R_{int} = 0.0436$, $R_{sigma} = 0.0608$]
Data/restraints/parameters	5521/0/415	6471/56/510
Goodness-of-fit on F^2 (S)	1.178	1.025
Final *R* indexes [$I >= 2\sigma(I)$]	$R_1 = 0.0290$, $wR_2 = 0.0950$	$R_1 = 0.0426$, $wR_2 = 0.0929$
Final *R* indexes [all data]	$R_1 = 0.0379$, $wR_2 = 0.1020$	$R_1 = 0.0667$, $wR_2 = 0.1037$
Largest diff. peak and hole (e $Å^{-3}$)	0.98/−0.68	1.15/−1.13

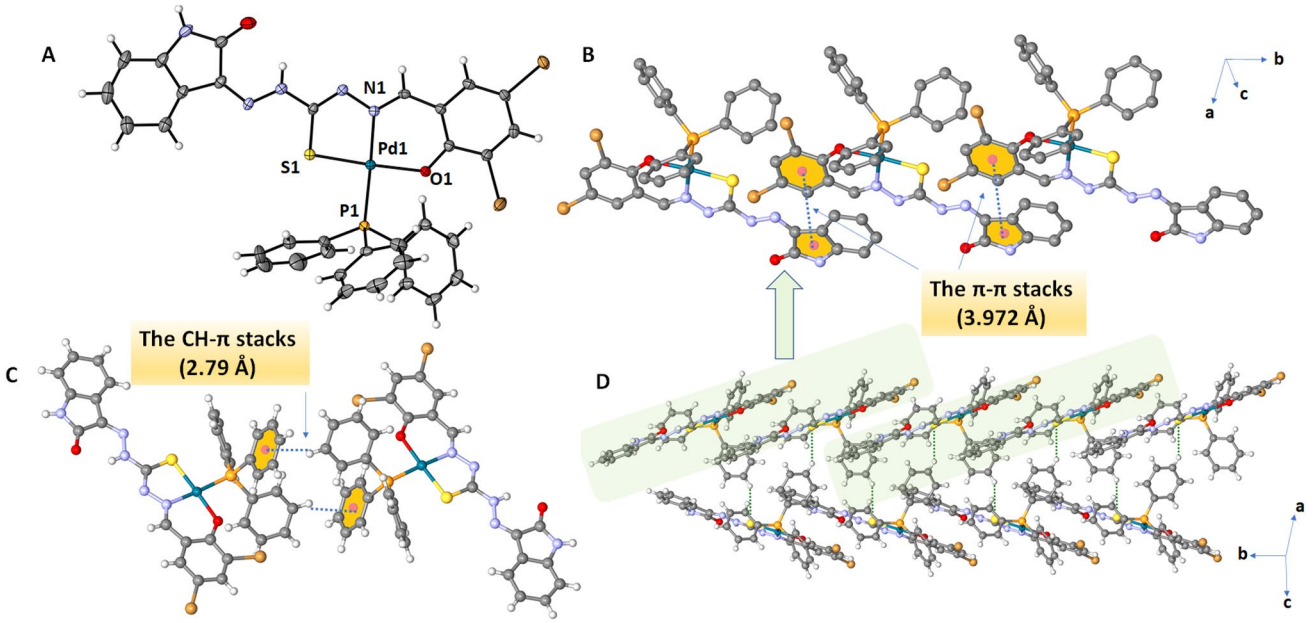

Fig. 1 **A** ORTEP drawings of the crystal structure of **Pd1** (30% probability level). All H-atoms are shown as small spheres of arbitrary radii. **B** Perspective view of the short $\pi\cdots\pi$ interactions in Pd1. **C** View of the CH$\cdots\pi$ interactions in Pd1. **D** View of the non-classical CH$\cdots$S contacts along the *b*-axis

complexes. These results are consistent with the complex structures we propose. Mass spectra of the complexes are given in Figures S9 and S10.

Crystallographic descriptions

The Pd(II) complexes (**Pd1** and **Pd3**) were confirmed unambiguously through single crystal X-ray diffraction analysis to better understand their solid-state structures. X-ray crystallographic data and refinement parameters for **Pd1** and **Pd3** were given in Table 1. Bond distances and angles were tabulated in Table 2. Crystallographic analysis exhibited that **Pd1** crystallizes in the monoclinic $P2_1/n$ space group. As shown in Fig. 1A, the asymmetric unit cell of **Pd1** consists of one 1-[2-oxoindolin-3-ylidene]-5-[3,5-dibromo-2-hydroxyphenyl) methylidene] thiocarbohydrazone (**1**), one Pd(II) metal cation, and one triphenylphosphine (PPh_3). **Pd1** metal center has a slightly distorted square planar coordination geometry through three donor atoms (S1, O1, N1) of **1** and one phosphorous atom (P1) of PPh_3 according to the geometric parameter ($\tau_4 = 0.05$), indicated by Yang et al. [86]. The nearly planar thiocarbohydrazone ligand (**1**) is tridentally coordinate to Pd(II), forming six- and five-membered chelate rings with O1–Pd1–N1 and S1–Pd1–N1 angles of 91.86 (10)° and 84.91 (8)°, respectively, and these angles agree with those observed in related Pd(II) complex [87–89]. The Pd–S, Pd–O, Pd–N and Pd–P bond distances are in the normal ranges and are well-matched to those found in four-coordinate Pd(II) complexes [90, 91]. The non-classical CH$\cdots$S (C32$\cdots$S1 = 3.795 Å, Fig. 1D) hydrogen bonding interactions lead a 1D chain structure with supporting $\pi\cdot\cdot\pi$ interactions (3.972 Å, Fig. 1B) between phenyl and indole rings along the *b*-axis in the crystal packing. Moreover, the CH$\cdots\pi$ interaction (C25–H25$\cdots$ π, d(H25$\cdots\pi$) = 2.79 Å, Fig. 1C) help to stabilize 3D crystal structure of **Pd1**.

Pd3 has a triclinic crystal system with P-1 space group. The asymmetric unit of **Pd3** comprises one 1-[2-oxoindolin-3-ylidene]-5-[3-bromo-5-chloro-2-hydroxyphenyl) methylidene]thiocarbohydrazone (**3**), one Pd(II) ion, one triphenylphosphine (PPh_3), and one DMF solvate. As illustrated in Fig. 2A, the tau-descriptor ($\tau_4 = 0.04$) exhibited that Pd(II) metal ion has no significant distortion of geometry, occupying by three donors (S1, O1, N1) of **3** and one P atom of PPh_3 to give a slightly distorted square planar coordination geometry. The thiocarbohydrazone ligand (**3**) is nearly planar and is in the same tridentate binding mode as in the **Pd1** complex, forming six- and five-membered chelate rings with O1–Pd1–N1 and S1–Pd1–N1 angles of 92.56 (13)° and 84.71 (10)°. The bond distances of Pd–S, Pd–O, Pd–N and Pd–P and angles around the Pd(II) coordination sphere are in the usual ranges when compared those with the literatures [90, 91]. Intermolecular CH$\cdots$Cl hydrogen bonding interaction (d(H3A$\cdots$Cl1) = 2.879 Å, Fig. 2B) less than sum of the corresponding van der Waals distance (r_{vdw}(Cl)) + r_{vdw}(H)) = 2.95 Å) links the two complexes through $R^2_2(8)$ hydrogen bond motif. This dimeric structure is further linked by CH$\cdots$Cl contacts d(H23$\cdots$Cl1 = 2.752 Å) to form 1D hydrogen-bonded chains along the *a*-axis in the crystal structure. The 1D chains are further stabilized through the

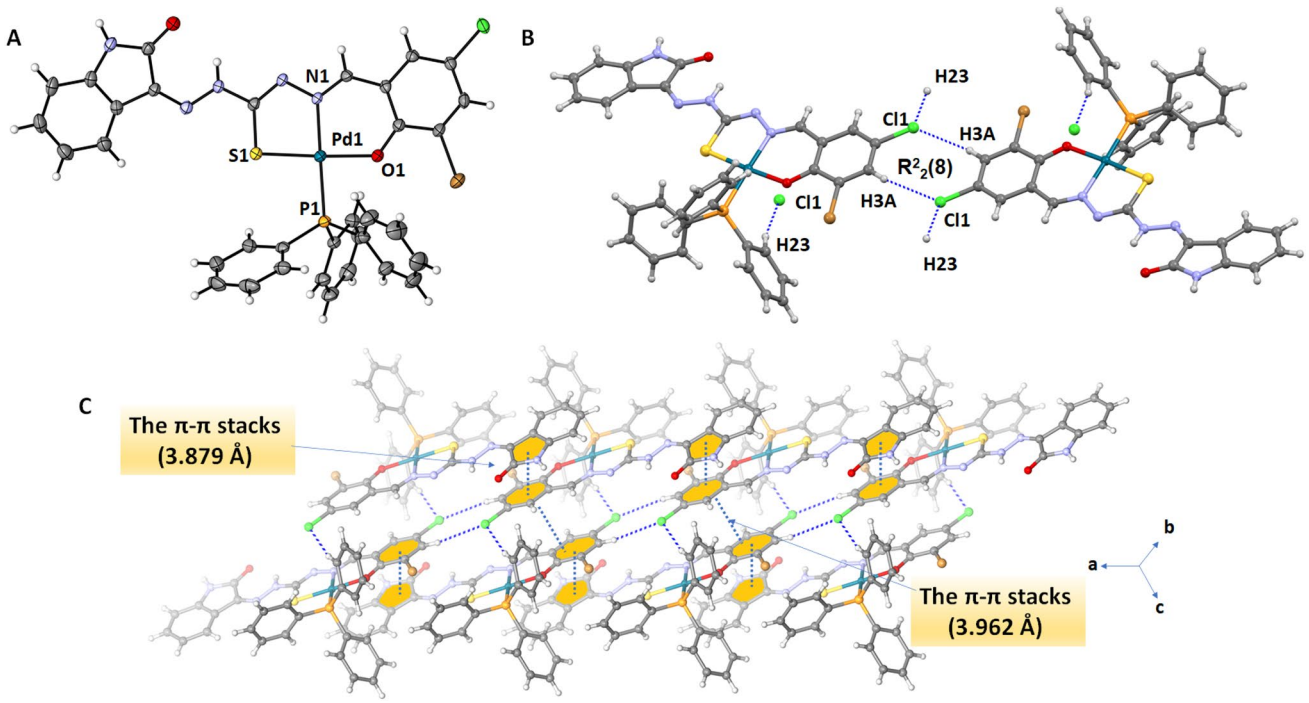

Fig. 2 **A** ORTEP drawings of the crystal structure of **Pd3** (30% probability level). All H-atoms are shown as small spheres of arbitrary radii. **B** Perspective view of the intermolecular CH···Cl hydrogen bonding interactions in **Pd3** along the *a*-axis. **C** View of the $\pi\cdots\pi$ interactions in **Pd3**

Table 3 Inhibition data of asymmetric isatin bisthiocarbohydrazone ligands (**1**–**3**) and their Pd(II) complexes (**Pd1**–**Pd3**) on AChE and hCA I, II isoforms

Compounds	IC_{50} (nM)						K_i (nM)		
	hCA I	r^2	hCA II	r^2	AChE	r^2	hCA I	hCA II	AChE
1	27.7	0.9798	19.3	0.9822	10.3	0.9940	14 ± 1.4	24 ± 1.9	30 ± 5.4
2	23.9	0.9813	17.8	0.9900	20.4	0.9845	9 ± 1.3	10 ± 1.2	28 ± 7.2
3	11.6	0.9862	6.0	0.9865	8.0	0.9931	7 ± 0.5	4 ± 0.3	22 ± 3.2
Pd1	9.1	0.9966	6.9	0.9941	4.9	0.9898	7 ± 1.0	21 ± 1.9	12 ± 1.1
Pd2	7.9	0.9829	5.9	0.9818	8.6	0.9850	9 ± 0.7	3 ± 0.3	10 ± 0.7
Pd3	6.2	0.9896	2.4	0.9898	3.6	0.9830	16 ± 2.2	7 ± 0.9	9 ± 0.6
AZA	34.1	0.9811	28.9	0.9806	–	–	29 ± 5.7	28 ± 6.0	–
TAC	–	–	–	–	39.1	0.9843	–	–	34 ± 3.6
Donepezil	–	–	–	–	33.5	0.9876			31 ± 6.2

Br···π (3.588(2) Å) and $\pi\cdots\pi$ interactions (3.879 Å, 3.962 Å, Fig. 2C). Also, DMF molecule forming moderate N–H···O hydrogen bonding interactions (N5···O3 = 2.729 Å) plays a key role in the formation of a 3D supramolecular network.

Biological studies

hCAs and AChE inhibition assay

In vitro inhibitory effects of asymmetric isatin bisthiocarbohydrazone ligands (**1–3**) and their Pd(II) complexes (**Pd1**–**Pd3**) on AChE, hCA I, and hCA II were determined using Ellman's [61] and Verpoorte's methods, respectively [55]. IC_{50} and K_i values of all compounds were calculated [92, 93].

All studied compounds inhibited hCA I more significantly than acetazolamide (AZA, K_i: 29 ± 5.7 nM) with the K_i values in the range of 7 ± 0.5 – 16 ± 2.2 nM (Table 3). Among the compounds **1**–**Pd3**, **Pd1** and **3** exhibited the most striking inhibition with the K_i values of 7 ± 1.0 and 7 ± 0.5 nM, respectively. When **1** and **2** are compared among themselves, the presence of chlorine substitutions in the structure showed a better inhibition property than bromine substitutions. On the other hand, when the Pd(II) complexes of **1** and **2** are compared, bromine substitutions showed a more effective

inhibition feature than chlorine substitutions. In **1**, an increase in the inhibition effect was observed as a result of the replacement of the bromine atom in the 5th position with chlorine (**3**, K_i: 7 ± 0.5 nM).

All compounds (**1**–**Pd3**) showed a potent inhibition effect on hCA II. K_i values of these compounds are in the range of 3 ± 0.3 – 24 ± 1.9 nM (Table 3). Among compounds **1**–**Pd3**, **Pd2** and **3** exhibited the most potent inhibition with the K_i values of 3 ± 0.3 and 4 ± 0.3 nM, respectively. As in hCA I inhibition, chlorine substitutions were more effective than bromine substitutions in hCA II inhibition. The **Pd2** inhibited the hCA II enzyme three times more than the hCA I enzyme. In **2**, an increase in the inhibition effect was observed as a result of the replacement of the chlorine atom in the 3rd position with bromine (**3**, K_i: 4 ± 0.3 nM).

Furthermore, compounds **1-Pd3** showed more remarkable AChE inhibitory effects than tacrine (TAC, K_i: 34 ± 3.6 nM) and donepezil (K_i: 31 ± 6.2 nM) with the K_i values in the range of 9 ± 0.6 – 30 ± 5.4 nM (Table 3). The **Pd3** and **Pd2** were determined as the most potent AChE inhibitors in this series with the K_i values of 9 ± 0.6 and 10 ± 0.7 nM, respectively. The **Pd1** caused a 2.5-fold increase in inhibition compared to **1**. The displacement of bromine and chlorine substitutions in **1** and **2** was not as effective as CA isoenzymes in the inhibition of the AChE enzyme. Pd(II) complexes showed a better inhibition effect in all the studied enzymes.

Conclusion

In this study, three new mixed ligand Pd(II) complexes were synthesized from the reaction of the asymmetric isatin bisthiocarbohydrazone ligands with $PdCl_2(PPh_3)_2$. Analytical and spectroscopic characterizations of the complexes were performed. Single crystals of the two complexes were obtained and their structures were elucidated by X-ray crystallography. Asymmetric bisthiocarbohydrazones served as the dibasic tridentate ONS donor ligand and replaced it by removing two chloride ions and one triphenylphosphine molecule from the starting complex. In the second part of the study, carbonic anhydrase I, II (hCAs) and acetylcholinesterase (AChE) inhibitory activities of the ligands and Pd(II) complexes were determined. The results clearly demonstrated that the ligands and their Pd(II) complexes effectively inhibited the used enzymes. This situation can be examined for the treatment of some diseases such as glaucoma and Alzheimer's, especially cancer, due to its connection with some metabolic diseases. More studies are needed on this subject to detail the structure–activity relationship and to recommend it as a drug. We think that our study will lead to new studies in the fields of Pd(II) complexes, thiocarbohydrazones and pharmacology.

Supplementary Information The online version contains supplementary material available at. https://doi.org/10.1007/s00775-022-01932-9.

Acknowledgements This work was supported by the Scientific Research Projects Coordination Unit of Istanbul University-Cerrahpaşa (Project Number FBA-2017-25859).

Declarations

Conflict of interest The authors declare that they have no conflict of interest.

References

1. Medvedev A, Buneeva O, Glover V (2007) Biol Targets Ther 1:151–162
2. Ozgun DO, Yamali C, Gul HI, Taslimi P, Gulcin I, Yanik T, Supuran CT (2016) J Enzyme Inhib Med Chem 31:1498–1501
3. Zhang YZ, Du HZ, Liu HL, He QS, Xu Z (2020) Arch Pharm 353:e1900299
4. Imada C (2004) Mar Biotechnol 6:193–198
5. Sonawane RP, Tripathi RR (2013) Int Lett Chem Phys Astron 7:30–36
6. Borad MA, Bhoi MN, Prajapati NP, Patel HD (2014) Synth Commun 44:897–922
7. Kumar SLA, Kumar MS, Jenniefer SJ, Muthiah PT, Sreekanth A (2013) Phosphorus Sulfur Silicon Relat Elem 188:1110–1118
8. Zafarian H, Sedaghat T, Motamedi H, Rudbari HA (2016) J Organomet Chem 825–826:25–32
9. Sathisha MP, Shetti UN, Revankar VK, Pai KSR (2008) Eur J Med Chem 43:2338–2346
10. Bonaccorso C, Grasso G, Musso N, Barresi V, Condorelli DF, La Mendola D, Rizzarelli E (2018) J Inorg Biochem 182:92–102
11. Metwally MA, Khalifa ME, Koketsu M (2012) Am J Chem 2:38–51
12. Bonaccorso C, Marzo T, La Mendola D (2020) Pharmaceuticals 13:1–19
13. Juranić Z, Anastasova F, Juranić I, Stanojković T, Radulović S, Vuletić N (1999) J Exp Clin Cancer Res 18:317–324
14. Gabr MT, El-Gohary NS, El-Bendary ER, El-Kerdawy MM, Ni N (2017) Eur J Med Chem 128:36–44
15. Sathisha MP, Revankar VK, Pai KSR (2008) Met Based Drugs 2008:1–11
16. Marques MPM (2013) Int Sch Res Not 2013:1–29
17. Özerkan D, Ertik O, Kaya B, Kuruca SE, Yanardag R, Ülküseven B (2019) Investig New Drugs 37:1187–1197
18. Bjelogrlić SK, Todorović TR, Kojić M, Senćanski M, Nikolić M, Višnjevac A, Araškov J, Miljković M, Muller CD, Filipović NR (2019) J Inorg Biochem 199:110758
19. Muche S, Harms K, Biernasiuk A, Malm A, Popiołek Ł, Hordyjewska A, Olszewska A, Hołyńska M (2018) Polyhedron 151:465–477
20. Shaheen F, Badshah A, Gielen M, Gieck C, Jamil M, de Vos D (2008) J Organomet Chem 693:1117–1126
21. Gaber M, El-Ghamry HA, Fathalla SK (2015) Spectrochim Acta A Mol Biomol Spectrosc 139:396–404

22. Rocha FV, Farias RL, Lima MA, Batista VS, Nascimento-Junior NM, Garrido SS, Leopoldino AM, Goto RN, Oliveira AB, Beck J (2019) J Inorg Biochem 199:110725
23. Rocha FV, Barra CV, Garrido SS, Manente FA, Carlos IZ, Ellena J, Fuentes ASC, Gautier A, Morel L, Mauro AE, Netto AVG (2016) J Inorg Biochem 159:165–168
24. Mitoraj MP, Michalak A (2010) Inorg Chem 49:578–582
25. Elsayed SA, Badr HE, di Biase A, El-Hendawy AM (2021) J Inorg Biochem 223:111549
26. Sağlık BN, Çevik UA, Osmaniye D, Levent S, Çavuşoğlu BK, Demir Y, Ilgın S, Özkay Y, Koparal AS, Beydemir Ş, Kaplancıklı ZA (2019) Bioorg Chem 91:103153
27. Caglayan C, Taslimi P, Türk C, Gulcin İ, Kandemir FM, Demir Y, Beydemir Ş (2020) Environ Sci Pollut Res 27:10607–10616
28. Hoff E, Zou D, Schiza S, Demir Y, Grote L, Bouloukaki I, Beydemir Ş, Eskandari D, Stenlöf K, Hedner J (2020) J Sleep Res 29:e12956
29. Bilginer S, Anıl B, Koca M, Demir Y, Gülçin İ (2021) Turk J Chem 45:805–818
30. Nar M, Çetinkaya Y, Gülçin İ, Menzek A (2013) J Enzyme Inhib Med Chem 28:402–406
31. Özbey F, Taslimi P, Gülçin İ, Maraş A, Göksu S, Supuran CT (2016) J Enzyme Inhib Med Chem 31:79–85
32. Kucuk M, Gulcin İ (2016) Environ Toxicol Pharmacol 44:134–139
33. Istrefi Q, Türkeş C, Arslan M, Demir Y, Nixha AR, Beydemir Ş, Küfrevioğlu Öİ (2020) Arch Pharm 353:e1900383
34. Tugrak M, Gul HI, Demir Y, Levent S, Gulcin I (2021) Arch Pharm 354:e2000375
35. Yamali C, Gul HI, Cakir T, Demir Y, Gulcin I (2020) Lett Drug Des Discov 17:1283–1292
36. Erdemir F, Celepci DB, Aktaş A, Taslimi P, Gök Y, Karabıyık H, Gülçin İ (2018) J Mol Struct 1155:797–806
37. Yamali C, Gül Hİ, Demir Y, Kazaz C, Gülçin İ (2020) Turk J Chem 44:1058–1067
38. Gülçin İ, Scozzafava A, Supuran CT, Koksal Z, Turkan F, Çetinkaya S, Bingöl Z, Huyut Z, Alwasel SH (2016) J Enzyme Inhib Med Chem 31:1698–1702
39. Bayrak C, Taslimi P, Karaman HS, Gulcin I, Menzek A (2019) Bioorg Chem 85:128–139
40. Günsel A, Taslimi P, Atmaca GY, Bilgiçli AT, Pişkin H, Ceylan Y, Erdoğmuş A, Yarasir MN, Gülçin İ (2021) J Mol Struct 1237:130402
41. Erdoğan M, Polat Köse L, Eşsiz S, Gülçin İ (2021) Arch Pharm 354:e2100113
42. Eruygur N, Koçyiğit UM, Taslimi P, Ataş M, Tekin M, Gülçin İ (2019) S Afr J Bot 120:141–145
43. Burmaoglu S, Yilmaz AO, Polat MF, Kaya R, Gulcin İ, Algul O (2019) Bioorg Chem 85:191–197
44. Yamali C, Gul HI, Ece A, Taslimi P, Gulcin I (2018) Chem Biol Drug Des 91:854–866
45. Kaya Y, Erçağ A, Uğuz Ö, Koca A, Zorlu Y, Hacıoğlu M, Tan ASB (2021) Polyhedron 207:115372
46. Burns GR (1968) Inorg Chem 7:277–283
47. Bruker (2014) APEX2, version 201411-0. Bruker AXS Inc, Madison
48. Bruker (2013) SAINT, version 834 A. Bruker AXS Inc, Madison
49. Bruker (2014) SADABS, version 2014/5. Bruker AXS Inc, Madison
50. Sheldrick GM (2015) Acta Crystallogr Sect A Found Adv 71:3–8
51. Sheldrick GM (2015) Acta Crystallogr Sect C Struct Chem 71:3–8
52. Dolomanov OV, Bourhis LJ, Gildea RJ, Howard JAK, Puschmann H (2009) J Appl Crystallogr 42:339–341
53. Spek AL (2009) Acta Crystallogr Sect D Biol Crystallogr 65:148–155
54. Macrae CF, Sovago I, Cottrell SJ, Galek PTA, McCabe P, Pidcock E, Platings M, Shields GP, Stevens JS, Towler M (2020) J Appl Crystallogr 53:226–235
55. Verpoorte JA, Mehta S, Edsall JT (1967) J Biol Chem 242:4221–4229
56. Huseynova M, Taslimi P, Medjidov A, Farzaliyev V, Aliyeva M, Gondolova G, Şahin O, Yalçın B, Sujayev A, Orman EB, Özkaya AR, Gulçin İ (2018) Polyhedron 155:25–33
57. Biçer A, Taslimi P, Yakalı G, Gülçin I, Gültekin MS, Cin GT (2019) Bioorg Chem 82:393–404
58. Akıncıoğlu A, Göksu S, Naderi A, Akıncıoğlu H, Kılınç N, Gülçin İ (2021) Comput Biol Chem 94:107565
59. Taslimi P, Caglayan C, Gulcin İ (2017) J Biochem Mol Toxicol 31:e21995
60. Scozzafava A, Kalın P, Supuran CT, Gülçin İ, Alwasel SH (2015) J Enzyme Inhib Med Chem 30:941–946
61. Ellman GL, Courtney KD, Andres V Jr, Featherstone RM (1961) Biochem Pharmacol 7:88–95
62. Turan B, Şendil K, Şengül E, Gültekin MS, Taslimi P, Gulcin I, Supuran CT (2016) J Enzyme Inhib Med Chem 31:79–88
63. Erdemir F, Celepci DB, Aktaş A, Gök Y, Kaya R, Taslimi P, Demir Y, Gulçin İ (2019) Bioorg Chem 91:103134
64. Pedrood K, Sherafati M, Mohammadi-Khanaposhtani M, Asgari MS, Hosseini S, Rastegar H, Larijani B, Mahdavi M, Taslimi P, Erden Y, Günay S, Gulçin İ (2021) Int J Biol Macromol 170:1–12
65. Demir Y, Duran HE, Durmaz L, Taslimi P, Beydemir Ş, Gulçin İ (2020) Appl Biochem Biotechnol 190:437–447
66. Demir Y, Taslimi P, Koçyiğit ÜM, Akkuş M, Özaslan MS, Duran HE, Budak Y, Tüzün B, Gürdere MB, Ceylan M, Taysi S, Gülçin İ, Beydemir Ş (2020) Arch Pharm 353:e2000118
67. Taslimi P, Akıncıoglu H and Gülçin İ (2017) J Biochem Mol Toxicol 31:e21973
68. Taslimi P, Gülçin İ, Öztaşkın N, Cetinkaya Y, Göksu S, Alwasel SH, Supuran CT (2016) J Enzyme Inhib Med Chem 31:603–607
69. Topal F, Gulcin I, Dastan A, Guney M (2017) Int J Biol Macromol 94:845–851
70. Gulcin İ, Alwasel SH (2022) Processes 10:132
71. Demir Y, Taslimi P, Ozaslan MS, Oztaskin N, Çetinkaya Y, Gulçin İ, Beydemir Ş, Goksu S (2018) Arch Pharm 351:e1800263
72. Demir Y, Işık M, Gülçin İ, Beydemir Ş (2017) Impact of HIV infection and HAART on serum lipids in men. J Biochem Mol Toxicol 31:e21936
73. Sujayev A, Garibov E, Taslimi P, Gulçin İ, Gojayeva S, Farzaliyev V, Alwasel SH, Supuran CT (2016) J Enzyme Inhib Med Chem 31:1531–1539
74. Ali OAM (2014) Spectrochim Acta A Mol Biomol Spectrosc 121:188–195
75. Geary WJ (1971) Coord Chem Rev 7:81–122
76. Abouzayed FI, Emam SM, Abouel-Enein SA (2020) J Mol Struct 1216:128314
77. Gray HB, Ballhausen CJ (1963) J Am Chem Soc 85:260–265
78. Yakan H, Bakır TK, Çavuş MS, Muğlu H (2020) Res Chem Intermed 46:5417–5440
79. Eğlence-Bakır S, Şahin M, Salt BZ, Tüzün E, Kara EM, Atun G, Çavuş S, Kızılcıklı İ (2020) Spectrochim Acta A Mol Biomol Spectrosc 237:118358
80. Bacchi A, Carcelli M, Pelagatti P, Pelizzi G, Rodriguez-Arguelles MC, Rogolino D, Solinas C, Zani F (2005) J Inorg Biochem 99:397–408
81. Gangarapu K, Manda S, Jallapally A, Thota S, Karki SS, Balzarini J, De Clercq E, Tokuda H (2014) Med Chem Res 23:1046–1056

82. Shabbir M, Akhter Z, Ashraf AR, Ismail H, Habib A, Mirza B (2017) J Mol Struct 1149:720–726
83. Shabbir M, Akhter Z, Ahmad I, Ahmed S, Shafiq M, Mirza B, McKee V, Munawar KS, Ashraf AR (2016) J Mol Struct 1118:250–258
84. Ayyannan G, Mohanraj M, Gopiraman M, Uthayamalar R, Raja G, Bhuvanesh N, Nandhakumar R, Jayabalakrishnan C (2020) Impact of HIV infection and HAART on serum lipids in men. Inorg Chim Acta 512:119868
85. Muralisankar M, Sujith S, Bhuvanesh NSP, Sreekanth A (2016) Polyhedron 118:103–117
86. Yang L, Powell DR and Houser RP (2007) Dalton Trans 9: 955–964
87. Halder S, Peng S-M, Lee G-H, Chatterjee T, Mukherjee A, Dutta S, Sanyal U, Bhattacharya S (2008) New J Chem 32:105–114
88. Ramachandran E, Raja DS, Bhuvanesh NSP, Natarajan K (2012) Dalton Trans 41:13308–13323
89. Kalaivani P, Prabhakaran R, Dallemer F, Poornima P, Vaishnavi E, Ramachandran E, Padma VV, Renganathan R, Natarajan K (2012) Metallomics 4:101–113
90. Prabhakaran R, Renukadevi SV, Karvembu R, Huang R, Mautz J, Huttner G, Subashkumar R, Natarajan K (2008) Eur J Med Chem 43:268–273
91. Prabhakaran R, Palaniappan K, Huang R, Sieger M, Kaim W, Viswanathamurthi P, Dallemer F, Natarajan K (2011) Inorg Chim Acta 376:317–324
92. Topal M, Gocer H, Topal F, Kalin P, Köse LP, Gülçin İ, Cakmak KC, Küçük M, Durmaz L, Gören AC, Alwasel SH (2016) J Enzyme Inhib Med Chem 31:266–275
93. Gulçin İ, Taslimi P, Aygün A, Sadeghian N, Bastem E, Kufrevioglu OI, Turkan F, Şen F (2018) Int J Biol Macromol 119:741–746

Authors and Affiliations

Yeliz Kaya[1] · Ayşe Erçağ[1] · Yunus Zorlu[2] · Yeliz Demir[3] · İlhami Gülçin[4]

[1] Inorganic Chemistry Division, Department of Chemistry, Faculty of Engineering, Istanbul University-Cerrahpaşa, 34320 Avcılar, Istanbul, Turkey

[2] Faculty of Science, Department of Chemistry, Gebze Technical University, 41400 Gebze, Kocaeli, Turkey

[3] Department of Pharmacy Services, Nihat Delibalta Göle Vocational School, Ardahan University, 75700 Ardahan, Turkey

[4] Department of Chemistry, Faculty of Science, Atatürk University, 25400 Erzurum, Turkey